Check for updates

Research Article

Advances in Mechanical Engineering

Advances in Mechanical Engineering
2019, Vol. 11(12) 1–9
© The Author(s) 2019
DOI: 10.1177/1687814019896927
journals.sagepub.com/home/ade
SAGE

Modeling and experimental research of quay crane cargo lowering processes

Tomas Eglynas[1], Arunas Andziulis[1], Marijonas Bogdevičius[2], Jolanta Janutėnienė[3], Sergej Jakovlev[1,3], Valdas Jankūnas[1], Audrius Senulis[1], Mindaugas Jusis[1,4], Paulius Bogdevičius[2] and Saulius Gudas[4]

Abstract

This article studies an operational problem arising at a container terminal. Klaipeda city port operations were surveilled up close and relevant remarks were made. The time efficiency of the existing container-lowering procedures using the simulation studies with a test-bed and with a real life crane operation was examined. Statistical analysis of the experimental results has showed that non-automated processes have higher time variance for the lowering process. The operations of quay crane for container handling "ship-to-shore" were analyzed, and lowering procedures time variations were determined. Each container is transported at operators own risk and with pre-defined time efficiency; therefore, it is hard to predict the optimal time for each container handling operation, thus, eventually, additional costs arise. Mathematical model was developed, which described dynamical characteristics of the container movement during lowering procedures. The lowering crane operation was modeled using known dynamic values for each separate case, and the complexity of the problem was proven. The results of modeling and experimental results show that it is possible to achieve optimal values with the existing processes.

Keywords

Dynamics modeling, quay crane, simulation, experimental research, container-lowering process, statistical analysis

Date received: 24 September 2019; accepted: 27 November 2019

Handling Editor: James Baldwin

Introduction

Intermodal shipping containers are widely adopted in the global transport chain to deliver various goods to end-users. Despite the obvious advantages, there is still plenty of room for improvements when it comes to time efficiency and quality increase. Global transport market is a network of companies and end-users, who rely on well-managed standards and systems. Recent trends and numbers suggest that about 90% of non-bulk global trade is being managed by shipping containers worldwide.[1,2] Europe alone in 2016 managed 0.8 billion tons of cargo.[3] Statistics shows that during the 10-year period between 2007 and 2017, shipping quantities increased by 66% (up to 148 million TEUs), taking into account the global merchandise trade by marine traffic.[4] Many engineers and managers worldwide foresaw such rapid increase. Yet, they could not manage it in an optimal manner. Thus, efficiency is a criterion which needs to be increased in order to adopt new challenges of the future. Cargo loading operations rely on loading and unloading speeds, safety of

[1]Klaipeda University, Klaipeda, Lithuania
[2]Vilnius Gediminas Technical University, Vilnius, Lithuania
[3]VSB-Technical University of Ostrava, Ostrava-Poruba, Czech Republic
[4]Cyber-Social Systems Engineering Group, Vilnius University, Vilnius, Lithuania

Corresponding author:
Tomas Eglynas, Klaipeda University, Herkaus Manto g. 84, LT-92294 Klaipeda, Lithuania.
Email: tmse@inbox.lt

Creative Commons CC BY: This article is distributed under the terms of the Creative Commons Attribution 4.0 License (https://creativecommons.org/licenses/by/4.0/) which permits any use, reproduction and distribution of the work without further permission provided the original work is attributed as specified on the SAGE and Open Access pages (https://us.sagepub.com/en-us/nam/open-access-at-sage).

operation,[5] and energy consumption in the vicinity of the port.[2] These factors tend to make final decisions when adopting new and untested technologies in practice.

The modernization of container terminals through modern ICT (information and communication technology) solutions partly solves the problems concerning the "Green" terminal initiative.[2] Autonomy of operations is adopted in many areas to control stability of container handling, transportation using terminal trucks, autonomous guided vehicle (AGV),[6] and so on. Even now, newly built cranes are using operator on site to manage the loading procedures.[7] Each new operator sees the loading standards as guidelines, but not strict rules. Therefore, crane autonomy[8] is necessary, in order to increase the efficiency of adopted standards and regulations, mechanical systems, and associated port investments. An autonomous quay crane is not an innovation on its own.[9] These complex systems already exist.[10] They are applied in many areas of industry including port operations.[11] However, modernization of existing infrastructure is a priority for most companies, working with container handling. More practical and real solution is to modernize existing systems, rather than purchase all new expensive infrastructure. Overall, there are crane stabilization systems that are already in use,[12] but they mostly lack of quality feedback and operator experience that makes huge impact on the efficiency of these expensive systems.[13]

In practice, the realization of complex control solutions is limited by the fluctuations of the spreader with load. Its movements are random in nature, due to external impacts, such as wind or physical contact with other objects.[14] It is difficult to predict such random deviations in practice. The most advanced European ports, such as Rotterdam or Hanover, the handling procedures and IT operations are mostly automated. However, the inclusion of the modern automated quay cranes is still an innovation for smaller ports throughout the world. In the light of the research and progress made in this area,[15–19] many ports in the world lack the application of these innovations.

Increasing the time efficiency of the cargo process is a topical issue addressed in the scientific work, for which various solutions are proposed, from management algorithms to cargo planning solutions.[2,6,20] The quay cranes are analyzed in the way of increasing loading time,[2,21] damping the load swinging during the loading–unloading process[21] using additional feedbacks in control system with the proportional–integral–derivative (PID) or proportional–integral (PI) controllers or using artificial intelligence analysis.[22,23]

The problem addressed in the port is the crane and the terminal truck synchronization means. The crane operator has to wait for the terminal truck or the terminal truck has to wait for the operator to finish his unloading routine. Due to constant operator faults, there is a delay in the end-of-shipment procedures. Especially, the container loading on terminal truck is managed difficultly. Authors propose to test analyze the lowering end procedure for the future control solution. The solution would use real terminal truck and spreader sensory data. Depending on the actual position of the terminal truck or the crane,[20] decisions are made systematically to slow down the speed of movement so that the target point reached at the same time by all involved bodies. This saves both energy resources and technical resources,[6] and increases crane and, consequently, the entire port efficiency.

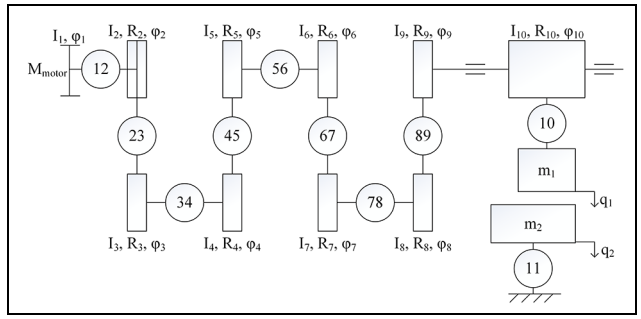

Figure 1. The overall dynamic model of the drive.

Mathematical modeling of container-lowering procedure by quay crane

The mathematical model of the quay crane was developed. The quay crane consists of asynchronous electrical motor, gears, shafts, drum, cables, container, and vehicle. Because the most important part was the end of container loading, the sway of container was not taken into account. The sway of container will be included in the future improved model. The structure of this model is shown in Figure 1.

In Figure 1, $I_1, \ldots, I_9$ are the mass moments of inertia; $R_2, \ldots, R_9$ are the radii; $\varphi_1, \ldots, \varphi_{10}$ are the angles (rotation angles); M_{motor} is the quay crane spreader lowering motor; q_1 and q_2 are the displacements; 12, 34, 56, 78 are the shafts; 10 is the cable; and 11 is the vehicle suspension.

In Figure 2(a), H is the cargo height, H_1 is the distance between road surface and drum axis, H_2 is the distance between road surface and vehicle platform, L is the cable length, and F_{12} is the contact force. In Figure 2(b), q_i and q_j are the generalized displacements, e is the number of element; k_e, c_e, and Δ_e are the stiffness, damping coefficients, and gap, respectively.

The mechanical system in question (Figure 2) consists of an electric motor (1), gears (2–9), cable, container, and terminal truck. Main parameters of the analyzed system in Figures 1 and 2 are 500 kW power

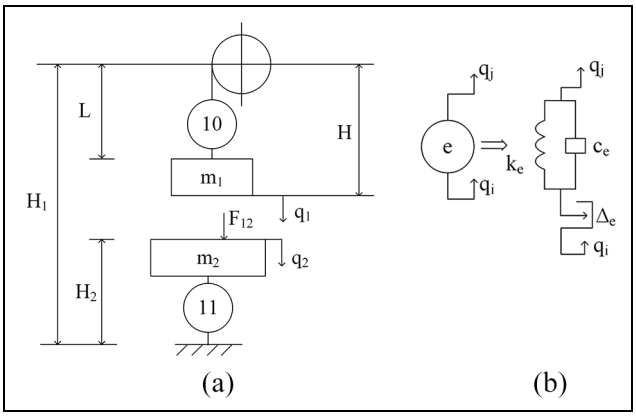

Figure 2. Container loading system design diagram: (a) dynamic model of spreader and transport, and cable (b) scheme of nonlinear element.

Table 1. The main parameters of transmission.

Parameter	Units	Value
Distance, H_1	m	11.0
Distance, H_2	m	1.50
Initial length of cable, L_0	m	2.0
Mass moment of inertia of rotor motor, I_1	kg m^2	2.0
Mass moment of inertia, I_2	kg m^2	0.0308
Mass moment of inertia, I_3	kg m^2	0.368
Mass moment of inertia, I_4	kg m^2	0.368
Mass moment of inertia, I_5	kg m^2	0.445
Mass moment of inertia, I_6	kg m^2	0.445
Mass moment of inertia, I_7	kg m^2	0.710
Mass moment of inertia, I_8	kg m^2	0.920
Mass moment of inertia, I_9	kg m^2	0.920
Mass moment of inertia, I_{10}	kg m^2	2.30
Mass of cargo and spreader, m_1	kg	22,572.0
Mass of vehicle, m_2	kg	10,000.0
Mass of 1 m cable, m_{L0}	kg	1.0
Modulus of elasticity of cable, E_L	GN/m^2	200.0
Cross section area of cable, A_L	m^2	3.1415E−4
Stiffness coefficient of contact, $k_{contact}$	MN/m	0.10E6
Damping coefficient of contact, $c_{contact}$	MN s/m	0.010E6
Integration time step	s	1.0E−6

in the main motor used for lowering container, $n = 995$ r/min, and frequency of $f = 50$ Hz. The main transmission parameters are given in Table 1.

The dynamics of the loading process are described in the equations below. Cargo distance from the axis of rotation of the drum $H(t)$, cable length $L(t)$, distance between the cargo and the terminal truck is $H_{12}(t)$ at any given time t is given in equation (1)

$$H(t) = L(t) + H_0, L(t) = L_0 + q_1(t), \quad H_{12}(t) = H_1 - H(t) - H_2 + q_2(t) \tag{1}$$

Here, h_0 is the height of the cargo. The rigidity coefficient of the cable is given in equation (2)

$$k_L(q_1) = \frac{E_L A_L}{L_0 + q_1(t)} \tag{2}$$

Here, E_L and A_L are the cable elastic modulus and cross-sectional area, respectively. The moment of inertia of the drum masses is given in equation (3)

$$I_{10} = I_{10,0} - r_{10}^2 m_{L0} L(t) \tag{3}$$

Here, m_{L0} is the mass per unit length of cable. The equations of motion of the load drive are derived using the second-order Lagrange equation (4)

$$\frac{d}{dt}\left(\frac{\partial E_K}{\partial q_j}\right) - \left(\frac{\partial E_K}{\partial q_j}\right) + \left(\frac{\partial E_P}{\partial q_j}\right) + \left(\frac{\partial D}{\partial q_j}\right) = Q_j \tag{4}$$

Here, E_k, E_P, and D are the kinetic energy of the drive, potential energy, and dissipative function, respectively; q_j and Q_j are the jth generalized coordinate and force, respectively. The torque of asynchronous motor M_{Motor} (the equation of variation) is given in equation (5)

$$\dot{M}_{Motor} = c_v\left(w_{M_0} - \dot{\phi}_1\right) - d_v M_{Motor} \tag{5}$$

Here, c_v and d_v are the asynchronous motor parameters, and w_{M0} is the motor rotor synchronic angular velocity. Asynchronous motor rotation (equation (6)) is given as

$$I_1\ddot{\phi}_1 = M_{Motor}(t) - M_b(t) - k_{12}(\phi_1 - \phi_2) - c_{12}\left(\dot{\phi}_1 - \dot{\phi}_2\right) - c_1\dot{\phi}_1 \tag{6}$$

Here, $M_b(t)$ is the engine braking torque; k_{12} and c_{12} are the shaft stiffness and resistance coefficients, respectively; and $\phi_1, \phi_2, \dot{\phi}_1, \dot{\phi}_2$ are the first and second body rotation angles and angular velocities. Second- and third-gear rotations (equations (7) and (8)) are

$$I_2\ddot{\phi}_2 = -k_{12}(\phi_2 - \phi_1) - c_{12}\left(\dot{\phi}_2 - \dot{\phi}_1\right) - k_{23}R_2u_{23} - c_2\dot{\phi}_2 \tag{7}$$

$$I_3\ddot{\phi}_3 = -k_{34}(\phi_3 - \phi_4) - c_{34}\left(\dot{\phi}_3 - \dot{\phi}_4\right) - k_{23}R_3u_{23} - c_3\dot{\phi}_3 \tag{8}$$

where

$$u_{23} = \delta_{23p}sign\left(\delta_{23p}\right) + \delta_{23m}sign(-\delta_{23m}) \tag{9}$$

$$\delta_{23p} = R_2\phi_2 + R_3\phi_3 - \Delta_{23} \ldots \Delta_{23} \tag{10}$$

Here, Δ_{23} is the gap between gears 2 and 3

$$\delta_{23m} = R_2\phi_2 + R_3\phi_3 + \Delta_{23} \tag{11}$$

Here, R_2 and R_3 are the radii of the main circles of the gears 2 and 3; $sign(x) = 1$, when $x>1$ and otherwise 0. The fourth- to ninth-gear rotations are calculated

similarly as the second and third. Tenth gear rotation equation is as equation (12)

$$\begin{aligned} I_{10}\ddot{\phi}_{10} = \dot{I}_{10}\dot{\phi}_{10} + \frac{1}{2}\frac{\partial I_{10}}{\partial \phi_{10}}\left(\dot{\phi}_{10}\right)^2 \\ - k_{910}(\phi_{10} - \phi_9) - c_{910}\left(\dot{\phi}_{10} - \dot{\phi}_9\right) \\ - c_{10}\dot{\phi}_{10} - R_{10}k_L(q_1)(R_{10}\phi_{10} - q_1) \\ - R_{10}c_{10}\left(R_{10}\dot{\phi}_{10} - \dot{q}_1\right) \end{aligned} \tag{12}$$

Cargo and vehicle movement equations (13) and (14) are

$$\begin{aligned} m_1\ddot{q}_1 = - \dot{m}_1\dot{q}_1 - k_L(q_1 - R_{10}\phi_{10}) \\ - c_L\left(\dot{q}_1 - R_{10}\dot{\phi}_{10}\right) + m_1 g - F_{12}sign(\delta_{12}) \\ + \frac{1}{2}(R_6\phi_6 - q_1)^2\left(\frac{E_L A_L}{L^2}\right) - c_{aer0}(\dot{q}_1)^2 sign(\dot{q}_1) \end{aligned} \tag{13}$$

$$m_2^{\cdot}q_2 = F_{12}sign(\delta_{12}) + m_2 g - k_2 q_2 - c_2\dot{q}_2 \tag{14}$$

Here, q_1, q_2 is the displacement of masses m_1 and m_2; m_1 and $\dot{m}_1$ are the cargo, spreader, and cable total mass and its derivative of time, respectively; c_L is the cable coefficient of resistance; and c_{aer0} is the aerodynamic force coefficient of resistance (equation (15))

$$\delta_{12} = (H_2 - q_2) - (H_1 - H(q_1)) \tag{15}$$

Here, m_2 is the vehicle mass, and k_2 and c_2 is the coefficients of vehicle suspension stiffness and resistance, respectively.

Thus, the mathematical model of quay crane was constructed and the results of container-lowering were examined for the comparison with the experimental data and giving implication of the possible lowering time reduction.

Experimental investigation

The aim of research was to test the real working conditions of the quay crane, operators work, the spreader efficiency, and unnecessary forces accumulated during container loading.[24] A simulation model was developed and tested. In recent years, researchers work closely with electrically powered terminal trucks and cranes.[25] In order to assess the need for synchronization, authors conducted experimental research in Klaipeda port. During the experimental research, the quay crane carried out loading operations, during which the data were collected. The practical experiment collected data from 204 real cycles of the loading process from ship to the quay and back again. MK2 data logger hardware was used for these experimental measurements (see Figure 3).

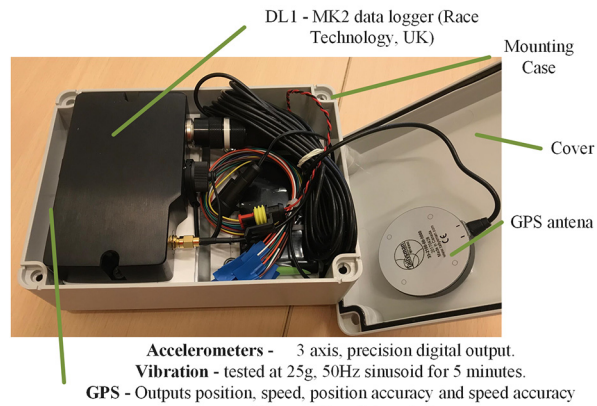

Figure 3. DL1-MK2 data logger (Race Technology, UK).

When determining the dynamic parameters of the object under investigation (in this case, the container), data about its acceleration, speed, and position in space were measured and recorded. For this purpose, a DL1-MK2 data logger (Race Technology, UK), a three-way accelerometer (guaranteed 2 g minimum full scale on both axes; resolution of 0.005 g; optional 6 g sensor available as a factory option) vibration measurements (vibration factory tested at 25 g, 50 Hz sinusoid for 5 min), was used to record and store vehicle motion dynamics parameters. For positioning, the meter is connected to a GPS antenna (GPS—outputs position, speed, position accuracy, and speed accuracy every 200 ms with no interpolation; GPS tracking loops optimized for applications up to about 4 g; tracking of all satellites in view). Based on the time course of the vehicle and the acceleration readings, the device measures the speed of the test object with an accuracy of 0.16 km/h, with a measurement error of up to 1%. Longitudinal and transverse accelerometers record accelerations up to 20 m/s^2 and measurement error up to 0.05 m/s^2.

After processing the data collected during the experimental measurements, the entire loading process was divided into stages to identify which technological loading process takes the longest. The purpose of this experiment was to identify problematic operations in the loading process when scheduling a synchronization task, thereby justifying the need for synchronization. By synchronizing individual port facilities (such as terminal trucks and quay cranes) and by planning cargo operations accordingly, it is possible to minimize the impact of these problem areas on the loading time. These stages and summarized experimental results are given in Table 2.

Experimental measurements were implemented when the cargo was shipped from the ship to the shore. Depending on the loading process, the operations are

Table 2. Statistical data of container loading time.

Stage of loading	Mean	Min	Max	Standard deviation	Variation coefficient (%)
1. Start of lifting (hooking)	2.43	0.62	11.47	1.84	76.01
2. Vertical lifting	4.68	1.04	13.47	3.32	70.89
3. Diagonal lifting	5.14	0.79	9.84	1.97	38.28
4. Horizontal transportation	6.34	2.05	19.03	3.46	54.68
5. Diagonal lowering	6.36	2.72	23.97	3.05	47.90
6. Vertical lowering	7.25	1.66	19.13	2.86	39.42
7. Placing on vehicle	5.43	2.36	20.43	2.99	55.16
Total (Ship-to-shore)	37.63	26.91	63.87	7.68	20.42

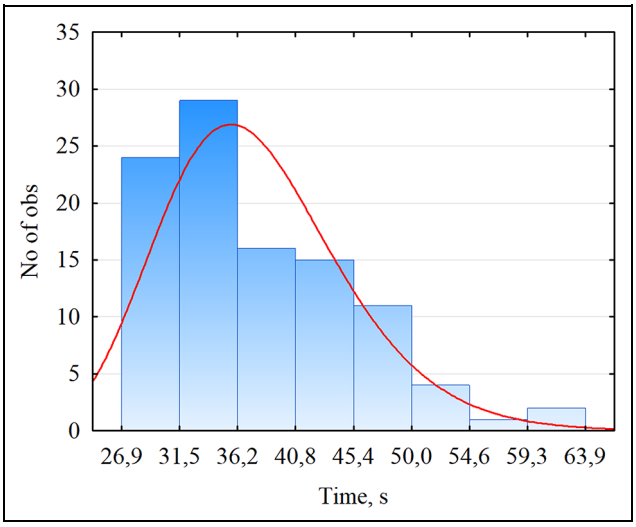

Figure 4. Histogram of experimental load from ship-to-ship on the quay.

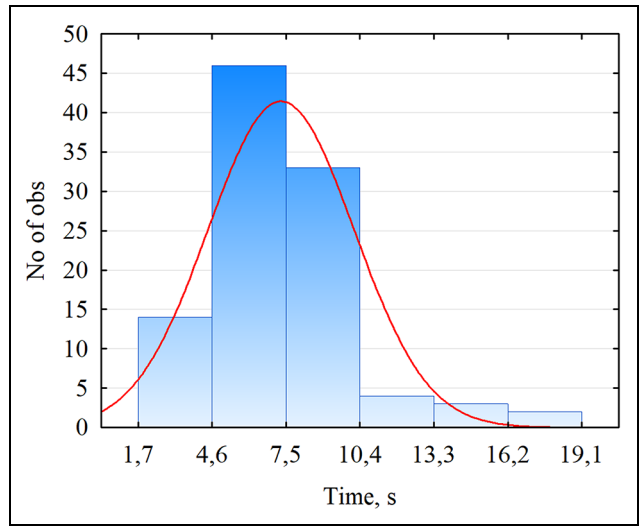

Figure 5. Histogram of experimental measurements of vertical lowering of container toward vehicle height.

divided into seven stages: (1) start of lifting (hooking), (2) vertical lifting, (3) diagonal lifting, (4) horizontal transportation, (5) diagonal lowering, (6) vertical lowering, and (7) placing on terminal truck. The overall loading cycle in the ship-to-shore process was also evaluated. The summarized results of experimental studies show that the entire duration of the ship-to-shore cycle of the loading process during the transfer of cargo from the ship to the shore is in accordance with statistical log-normal law.

The number of data $n = 102$ was measured (from ship to shore). The log-normal law hypothesis was tested by Pearson's χ^2 criterion. The histogram of the experimental loading times determined during experimental measurements is shown in Figure 4.

After analyzing the loading process measurements in stages, steps 6 and 7 were chosen for further analysis, that is, vertical lowering and positioning on the vehicle. These stages determine the crane-to-vehicle alignment to optimize the loading process and make it continuous. In Figure 5, the distribution of the vertical lowering time is presented.

We can see that the vertical lowering mean time of the container t is equal to 7.3 s, and the vertical lowering height mean value is 8.8 m, considering the standard deviation as 4.5 m. Hypothesis of lowering time distribution by Normal law was tested by Pearson's χ^2 criterion. Experimental results show that the average weight of the container load during the experimental measurements is 22.2 ton and the standard deviation is 10.2 ton, and coefficient of variation is 46%. In Figure 6, the distribution of the loading phase duration is presented, when the load is placed on the terminal truck and detached.

As we can see shorter intervals predominate, they represent about 50% of the total ($n = 102$) measurement result. Average is about 5.43 s; however, container placement can take up to 20 s. Duration of this step could be optimized by automation of loading process, and this process could be about 2 s, as show experimental results. The purpose of the synchronization task is to make the vehicle arrive when the load lowered during the loading process. Therefore, experimental measurements carried out when the equipment mounted on a container transport. Experimental research measured

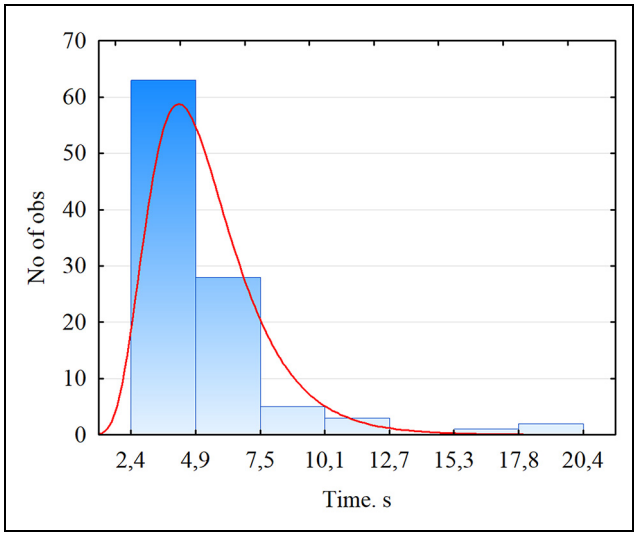

Figure 6. Histogram of experimental measurement container placement on terminal vehicle.

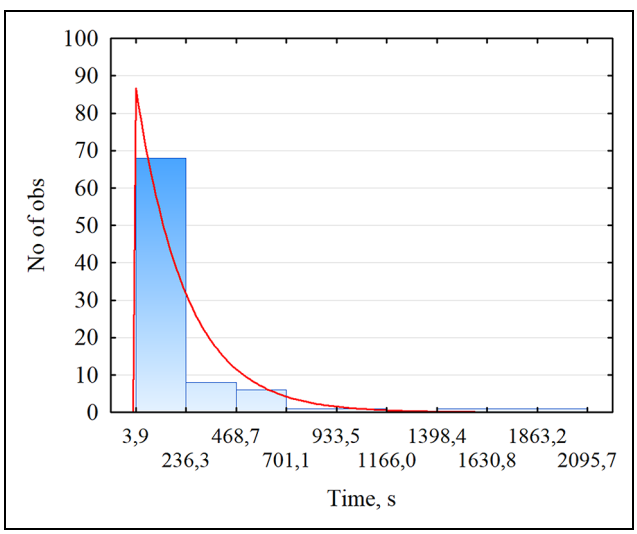

Figure 7. Histogram of experimental measurements of vehicle waiting time.

the trajectory of the terminal truck in the port area and its waiting time at the crane (see Figure 7).

The results show that the waiting time of the vehicle at the container crane varies from 4 s to 34 min (2096 s). The average waiting time is 229 s and standard deviation 346 s. The process is extremely unstable with a coefficient of variation of more than 150%. During the experimental measurements, the cargo was also evaluated (when mounting the equipment on the gripper—the closest point to the container). During these experimental measurements, the velocities and accelerations of the moving load were measured. After processing the results, we selected the best result—the experimental result of the fastest lowering of the load (see Figure 8).

The results show that investigated case of load lowering vertically was done in 1.9 s. The lowering speed of this situation is given in Figure 8(a). As a result, speed values are negative because the load is lowered. We also watched the fluctuations of the load that influence the full automation of the process. The load fluctuations in the horizontal plane during lowering are shown in Figure 8(b). As one can notice, container sways in a 10 cm boundary. This value suggests that the cargo lowered in a stable manner and no outer forces affect the sway (wind gusts or operator mistakes).

The experimental results show the need of more sophisticated control of the crane–container terminal truck system, but to work in real situation and to improve the performance are difficult due to the intervention into the port operation. Therefore, the mathematical model for lowering the container was developed to make adequate modeling and producing the tool for control system development.

Results and discussion

During the numerical simulation, the cargo lowering process was analyzed, which corresponds to the loading stage 6 of the experimental investigations. Simulation of the lowering process was completed by evaluating the force during contact placing the load on the vehicle. The results of numerical simulation are presented in Figure 9.

During numerical simulation, the load was lowered vertically down (see in Figure 9(a)). Due to the high weight of the load and the elasticity of the cable, the damping occurs. Figure 10 shows the situation when the load is placed on a vehicle with a dynamic force F12 of ~180 kN (see Figure 9(b)).

Changes of torque moment of the gear wheels during lowering presented in Figure 10.

During the modeling phase, the gap between the gear teeth was estimated. As we see during the lowering of the load, it has a negative effect; it excites the vibrations of the gears. This affects the lowering process; the vibrations pass to the cable and consequently worsen the loading conditions. Figure 11 shows the acceleration during horizontal lowering, and in Figure 11(a), the numerical simulations show that the acceleration values increase significantly when cargo has a contact with terminal truck. This is consistent with experimental measurements (Figure 11(b) (point 7)), with a significant increase in acceleration values and excitation of the terminal truck when the load is applied. On comparison, the results with the best experimental data that was achieved during the lowering (b) – was 2.4 s, but modeling results show that it is – in ideal conditions – possible to make the operation in 0.5 s (a). And, the results are comparable in time and amplitude, thus

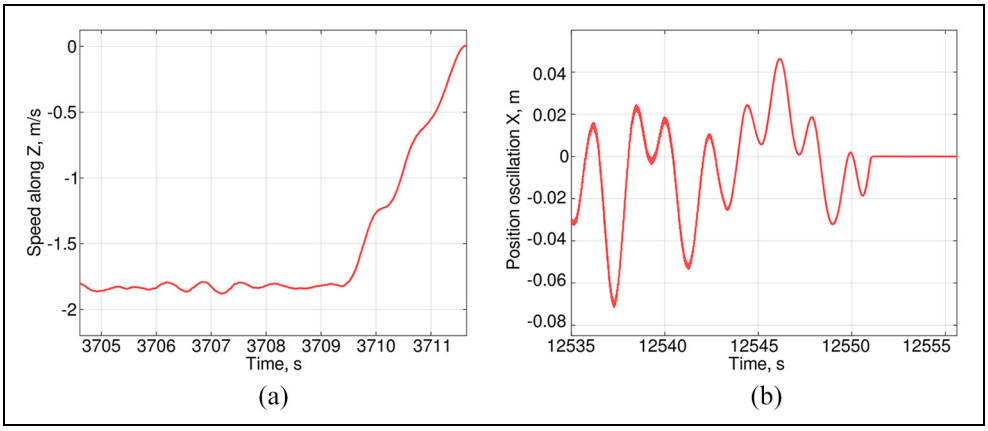

Figure 8. Experimentally measured data: (a) the speed of the vehicle in the *z*-direction when the load lowered vertically and (b) container sway in horizontal plane during lowering.

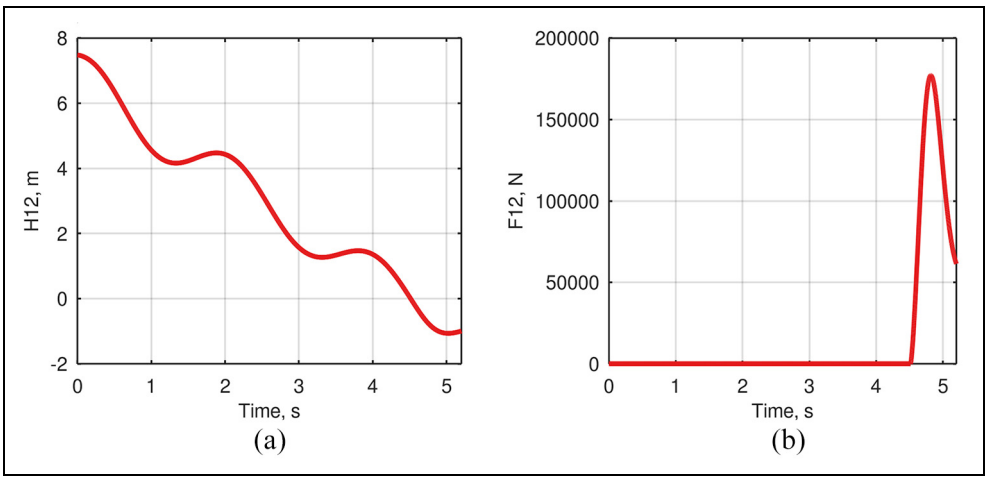

Figure 9. The result of numerical simulation: (a) variation of the vertical distance *H* of the load to the vehicle and (b) variation of impact force during loading.

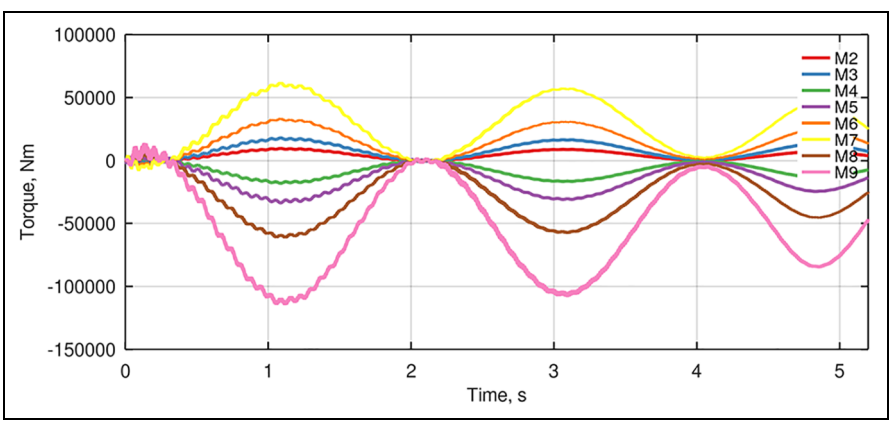

Figure 10. Numerical simulation result: torques during load lowering.

approving the model adequacy. So, the mean time of last stage of lowering of container could be moved toward the range of 0.5–2.5 s.

Figures above demonstrate that when the container is placed on the terminal truck, additional dynamic force is added, which at sometimes can be twice as large

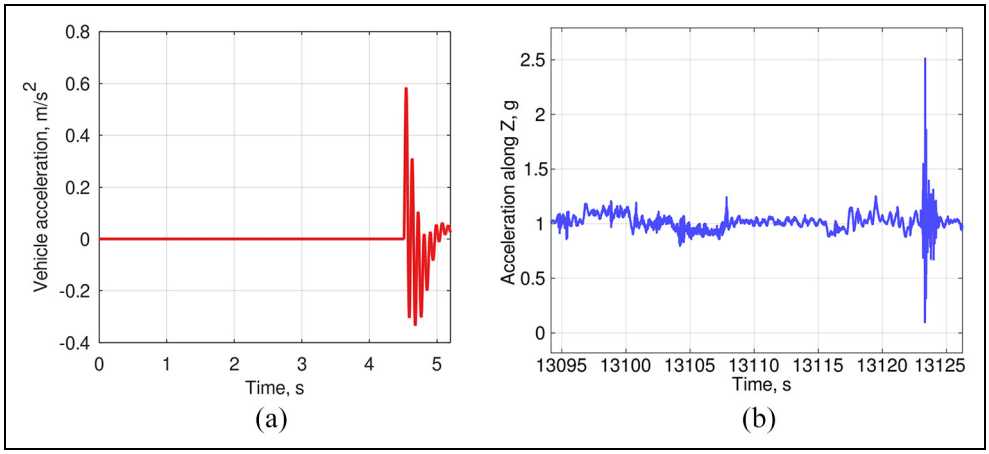

Figure 11. Numerical modeling (a) and experiment (b) results comparison.

as the levering container weight. This is a known effect in classical mechanics. Such regularity is confirmed by the results of numerical simulation and experimental acceleration measurements (see Figure 11). Experimental measurements show a very similar tendency during container loading procedures.

Conclusion

In this article, as a result, we demonstrate the generalization of the measurements with real quay crane and terminal vehicle and propose a mathematical model describing the dynamic properties of both. Experimental measurements "in situ" of container-lowering to terminal truck have been investigated in detail and statistical analysis of the new experimental results carried out. Experimental measurements showed that variance coefficient reached up to 150% on final handling operation. These operation durations varied between 2.36 and 20.43 s, with a mean value of 5.43 s. The entire lowering cycle variation coefficient reached 55.16%. Shorter time boundary shows that the handling process is optimizable up to two times by scheduling the operations between quay crane and terminal truck operators and using specialized algorithms for lowering process control for each individual case. This in fact could provide stability to port operations and make processes and procedures more agile for long-term planning. According to these new experimental data and research findings, further plans will be prepared to develop a methodology for crane and terminal truck, AGV synchronization in real time and will be used to bridge the scheduling mechanisms into a single real-time synchronization system.

Acknowledgements

The authors thank other project (No. 01.2.2-LMT-K-718-01-0081) members: Dr R Didziokas, Dr E Guseinoviene, Dr M Kurmis, Dr D Drugnilas, and Z Lukosius for valuable insights and collection of data on site.

Declaration of conflicting interests

The author(s) declared no potential conflicts of interest with respect to the research, authorship, and/or publication of this article.

Funding

The author(s) disclosed receipt of the following financial support for the research, authorship, and/or publication of this article: This research was funded by the European Regional Development Fund according to the supported activity "Research Projects Implemented by World-class Researcher Groups" under Measure No. 01.2.2-LMT-K-718-01-0081.

ORCID iD

Tomas Eglynas https://orcid.org/0000-0002-9973-5896

References

1. Clausen U, Kaffka J and Meier F. CONTSIM—container terminal management with simulation. *Procedia: Soc Behav Sci* 2012; 54: 332–340.
2. Kavakeb S, Nguyen TT, McGinley K, et al. Green vehicle technology to enhance the performance of a European port: a simulation model with a cost-benefit approach. *Transp Res Part C Emerg Technol* 2015; 60: 169–188.
3. European Commission. *Annex to motorways of the sea detailed implementation plan*, 2018, https://vayla.fi/documents/20473/465955/Final-II-MoS-study-2018-2+Annex.pdf/9cbe31a9-afde-4c79-9370-394bc864ffa5
4. Benamara H. Role of international shipping. In: *UNCTAD multiyear expert meeting on transport, trade logistics and trade facilitation*, Geneva, 21–23 November 2018, p.13. Geneva: United Nations Conference on Trade and Development.

5. Speier C, Whipple JM, Closs DJ, et al. Global supply chain design considerations: mitigating product safety and security risks. *J Oper Manag* 2011; 29: 721–736.
6. Xin J, Negenborn RR and Lodewijks G. Trajectory planning for AGVs in automated container terminals using avoidance constraints: a case study. *IFAC Proc Vol* 2014; 47: 9828–9833.
7. Hong KS and Ngo QH. Dynamics of the container crane on a mobile harbor. *Ocean Eng* 2012; 53: 16–24.
8. Zheng K, Lu Z and Sun X. An effective heuristic for the integrated scheduling problem of automated container handling system using twin 40' cranes. In: *Proceedings of the 2010 second international conference on computer modeling and simulation*, Sanya, China, 22–24 January 2010, pp.406–410. New York: IEEE.
9. Zhen L, Hu H, Wang W, et al. Cranes scheduling in frame bridges based automated container terminals. *Transp Res Part C Emerg Technol* 2018; 97: 369–384.
10. Alasali F, Haben S and Holderbaum W. Stochastic optimal energy management system for RTG cranes network using genetic algorithm and ensemble forecasts. *J Energy Storage* 2019; 24: 100759.
11. Papaioannou V, Pietrosanti S, Holderbaum W, et al. Analysis of energy usage for RTG cranes. *Energy* 2017; 125: 337–344.
12. Liu D and Ge YE. Modeling assignment of quay cranes using queueing theory for minimizing CO_2 emission at a container terminal. *Transp Res Part D Transp Environ* 2018; 61: 140–151.
13. Bichou K. An empirical study of the impacts of operating and market conditions on container-port efficiency and benchmarking. *Res Transp Econ* 2013; 42: 28–37.
14. Arena A, Lacarbonara W and Casalotti A. Payload oscillations control in harbor cranes via semi-active vibration absorbers: modeling, simulations and experimental results. *Procedia Engineer* 2017; 199: 501–509.
15. Tuan LA, Cuong HM, Trieu P, et al. Adaptive neural network sliding mode control of shipboard container cranes considering actuator backlash. *Mech Syst Signal Process* 2018; 112: 233–250.
16. Sha M, Zhang T, Lan Y, et al. Scheduling optimization of yard cranes with minimal energy consumption at container terminals. *Comput Ind Eng* 2017; 113: 704–713.
17. Ileš Š, Matuško J and Kolonić F. Sequential distributed predictive control of a 3D tower crane. *Control Eng Pract* 2018; 79: 22–35.
18. Verdés Kairuz RI, Aguilar LT, de Loza AF, et al. Robust positioning control law for a 3D underactuated crane system. *IFAC-PapersOnline* 2018; 51: 450–455.
19. Zhang M, Zhang Y, Chen H, et al. Model-independent PD-SMC method with payload swing suppression for 3D overhead crane systems. *Mech Syst Signal Process* 2019; 129: 381–393.
20. Li B, Liu H, Xiao D, et al. Centralized and optimal motion planning for large-scale AGV systems: a generic approach. *Adv Eng Softw* 2017; 106: 33–46.
21. Güven C and Eliiyi DT. Trip allocation and stacking policies at a container terminal. *Transp Res Proc* 2014; 3: 565–573.
22. Sun Z, Wang N, Bi Y, et al. A DE based PID controller for two dimensional overhead crane. In: *Proceedings of the 34th Chinese control conference*, Hangzhou, China, 28–30 July 2015, pp.2546–2550. New York: IEEE.
23. Jaafar HI, Mohamed Z, Abidin AFZ, et al. PSO-tuned PID controller for a nonlinear gantry crane system. In: *Proceedings of the 2012 IEEE international conference on control system, computing and engineering (ICCSCE 2012)*, Batu Ferringhi, Malaysia, 23–25 November 2012, pp.515–519. New York: IEEE.
24. Park KP, Cha JH and Lee KY. Dynamic factor analysis considering elastic boom effects in heavy lifting operations. *Ocean Eng* 2011; 38: 1100–1113.
25. Bahnes N, Kechar B and Haffaf H. Cooperation between intelligent autonomous vehicles to enhance container terminal operations. *J Innov Digit Ecosyst* 2016; 3: 22–29.